

<https://doi.org/10.1038/s43247-026-03427-w>

Collapse of the Atlantic meridional overturning circulation would lead to substantial oceanic carbon release and additional global warming

Check for updates

Da Nian ¹ ✉, Matteo Willeit ¹, Nico Wunderling^{1,2}, Andrey Ganopolski¹ & Johan Rockström ^{1,3}

The potential collapse of the Atlantic Meridional Overturning Circulation could profoundly impact regional and global climates, yet its effects on the carbon cycle and subsequently global temperature remain seriously underexplored. Here we quantify carbon cycle responses across different background global warming levels using a fast Earth system model. We find that Atlantic Meridional Overturning Circulation collapse increases atmospheric carbon dioxide by 47–83 ppm carbon dioxide, leading to around 0.2 °C of additional global warming at higher carbon dioxide background levels after offsetting ocean-dynamics-driven cooling. Despite the modest global warming effect, regional temperature anomalies are pronounced: Arctic temperatures cool by ~ 7 °C (60 °N–90 °N), while Antarctic temperatures warm by ~ 6 °C (60 °S–90 °S). This latter response originates from deep convection triggered in the Southern Ocean, which ventilates deep carbon-rich waters. Such long-term equilibrium responses reveal key physical and carbon-cycle mechanisms and highlight substantial regional climate risks associated with an Atlantic Meridional Overturning Circulation collapse.

As global warming continues, limiting the growth of atmospheric carbon dioxide (CO₂) concentration has become an urgent priority. In 2024, global mean surface temperature (GMT) has exceeded 1.5 °C above pre-industrial levels^{1–3} signaling a potential long-term breach of this threshold within the next two decades jeopardizing the Paris Agreement goal of limiting long-term warming below 1.5 °C³. Therefore, beyond reducing anthropogenic emissions, such as following a carbon law to have a chance of achieving carbon neutrality⁴, it is crucial to quantify the impact of climate change on the natural carbon sinks on land and the ocean⁵. The ocean is a vital carbon reservoir, and has absorbed approximately one quarter of anthropogenic CO₂ emissions over recent decades⁶, with recent estimates indicating about 26% for 2013–2022⁷. While projected ocean and land carbon sinks increase, the proportions of absorbed CO₂ are smaller in scenarios with higher emissions, resulting in a larger fraction of emitted CO₂ remaining in the atmosphere⁸. Changes in major ocean circulation patterns in the future could have substantial implications for the global carbon budget⁹.

The Atlantic Meridional Overturning Circulation (AMOC) is considered to be one of the climate tipping elements that can have multiple

equilibrium states¹⁰. This goes back to Stommel et al. (1961)¹¹, who, using a simple box model, proposed that the AMOC has two different stable equilibrium states due to a positive salt advection feedback. Subsequent studies have further identified the bistability of the AMOC in modeling simulations, indicating the possibility of a stable AMOC collapsed state^{12–16}. AMOC collapse has been shown to have a profound effect on climate^{17–21}. Paleoclimate data provide strong evidence that AMOC changes caused abrupt climate changes during glacial periods^{22–24}. Although the mechanisms of glacial climate changes are different from those caused by anthropogenic emissions, model simulations show that global warming may cause a weakening and even a complete shutdown of the AMOC in the future^{25–28}. Despite no significant signal from direct observational measurements²⁹, some studies based on indirect proxies suggest that the AMOC is weakening, and is currently in its weakest period in a thousand years³⁰, although the reliability of such reconstructions is still debated³¹. The IPCC AR6 concludes that, with medium confidence, AMOC shutdown is unlikely this century³². However, recent research suggests this risk may be underestimated, highlighting the potential for substantial, persistent global

¹Earth System Analysis and Earth Resilience Science Unit, Potsdam Institute for Climate Impact Research (PIK), Member of the Leibniz Association, Potsdam, Germany. ²Center for Critical Computational Studies (C3S), Goethe University Frankfurt, Frankfurt am Main, Germany. ³Institute of Environmental Science and Geography, University of Potsdam, Potsdam, Germany. ✉e-mail: danian@pik-potsdam.de

impacts if tipping points were crossed^{20,33,34}. Modeling studies also show that the weakening or shutdown of the AMOC can affect the functioning of the marine carbon cycle and cause additional changes in CO₂^{35–37}.

Most previous studies on the impact of an AMOC collapse focus on the induced climate changes under pre-industrial conditions^{20,37–39} or specific CO₂ levels¹⁸, finding that it causes a substantial drop in overall global surface temperatures, especially in the Northern Hemisphere, with a slight warming in the Southern Hemisphere. Several studies have investigated the transient AMOC response to ongoing CO₂ forcing (e.g., SSP8.5 scenarios or transient CO₂ experiments), indicating a weakening with increased CO₂ forcing and a potential collapse at higher concentrations. Here, we define collapse as a rapid weakening of the AMOC to a nearly complete shutdown with the maximum strength below 5 Sv. These studies consistently show that AMOC weakening or collapse results in a similar global cooling pattern^{40–42}. Several modelling studies for glacial and interglacial periods suggest that AMOC weakening or shutdown may result in increases or decreases in CO₂, depending on model structure and boundary conditions, reflecting the complex interplay and compensating effects among ocean circulation changes and terrestrial carbon response³⁷. As a result, the CO₂ response to an AMOC shutdown remains highly uncertain. On the other hand, varying equilibrium CO₂ concentrations substantially influence AMOC stability, with higher CO₂ levels potentially corresponding to stronger equilibrium AMOC strength^{27,43,44}, yet the consequences of AMOC shutdown on the climate and carbon cycle under these conditions remain understudied.

To simulate the impact of an AMOC collapse on climate under different global warming levels, we use the fast Earth System Model CLIMBER-X because it is computationally efficient and can systematically analyze the impact of an AMOC shutdown on climate and the carbon cycle^{45,46}. CLIMBER-X includes a 3D ocean model, a statistical-dynamical atmosphere model, a thermodynamic-dynamic sea ice model, an ocean biogeochemistry model and a land surface model with dynamic vegetation and can simulate the global carbon cycle and the evolution of atmospheric CO₂⁴⁵. The climate sensitivity of the model is ~3 °C and as such comparable to other major General Circulation Models⁸. We focus on the impact of an AMOC collapse at different equilibrium warming levels, and the resulting changes in the ocean and land carbon cycles and their impacts on the global climate via changes in atmospheric CO₂. We designed experiments to quantify the role of ocean and land carbon cycles by setting up: (1) a coupled system with fully interactive CO₂ (fully coupled, including the full land and ocean carbon cycle), (2) a version with the land carbon cycle disabled, leaving an ocean-only carbon cycle (land-carbon-off), and (3) a fixed-CO₂ version to estimate the pure climate response following the AMOC shutdown (fixed-CO₂). To force an AMOC collapse we apply freshwater hosing from model year 1000 to 2000, followed by continued simulation until year 7000. We add the freshwater to the Atlantic surface between 50 °N and 70 °N with intensities of 0.1 Sv and 0.2 Sv and compensate by adding a spatially uniform salt flux to the tropical Pacific between 30 °S and 30 °N to conserve global mean salinity (Fig. 1). To investigate the effect of an AMOC collapse at various warming levels we perform experiments starting from the climate and carbon cycle in equilibrium with CO₂ concentrations ranging from 280 ppm to 600 ppm. Before starting the hosing experiments we spin up the model for 10,000 years, guaranteeing that the background conditions are in equilibrium across different CO₂ levels (See Method and Supplementary Fig. 1).

Results

AMOC response to hosing at different CO₂ levels

After conducting 10,000-year spin-up simulations under prescribed atmospheric CO₂ concentrations ranging from 280 to 600 ppm, the system reaches equilibrium at each baseline CO₂ level (Supplementary Fig. 1). In the pre-industrial (280 ppm baseline) experiment, the simulated AMOC (Supplementary Fig. 2c) is slightly deeper and stronger than in many CMIP-class models⁴⁷ but remains within the range of observational estimates^{47,48}. We also compared our pre-industrial global overturning streamfunction with that from CMIP5 models and found similar large-scale patterns

(Supplementary Fig. 3), consistent as well with reanalysis-based estimates⁴⁹. The equilibrium AMOC increases in CLIMBER-X with higher CO₂ (Supplementary Fig. 4b), which does not contradict the weakening of AMOC in transient CO₂ experiments⁵⁰. Willeit and Ganopolski (2024)⁴³ show that in the CLIMBER-X model, higher CO₂ levels enhance North Atlantic surface buoyancy losses primarily through thermal effects, which favors convection and deep water formation, thereby strengthening the AMOC. This is consistent with other atmosphere-ocean general circulation model simulations, suggesting that after an initial weakening due to transient warming, the AMOC may recover above its original strength due to positive salinity anomalies in the North Atlantic and long-term warming in the low-latitude Atlantic, which together enhance the meridional density gradient and strengthen the AMOC²⁷. This interpretation does not exclude the well-established role of Southern Ocean wind-driven upwelling in setting the long-term equilibrium strength of AMOC, which requires compensating downwelling in the Atlantic or Pacific^{51,52}.

Starting from these different equilibrium states, we apply freshwater hosing, utilizing the three model setups: fully coupled, land-carbon-off, and fixed CO₂.

The results of the hosing experiments in the fully coupled model setup show the monostable and bistable characteristics of AMOC under different CO₂ levels (Fig. 1a). For the pre-industrial CO₂ level of 280 ppm the AMOC shows monostable behavior by collapsing under freshwater hosing but fully recovering once the forcing ends. At CO₂ levels of 350 ppm or higher, the system shows bistable behavior, meaning that once the AMOC collapses, it cannot recover and stays in the off state. However, higher CO₂ scenarios need a stronger freshwater hosing to cause this collapse. The corresponding results are also presented in the land-carbon-off and fixed CO₂ model setups (Supplementary Fig. 5). Willeit and Ganopolski (2024)⁴³ demonstrate using the CLIMBER-X model that atmospheric CO₂ is a crucial control variable alongside freshwater forcing in determining AMOC stability. They show that when CO₂ exceeds 350 ppm, the AMOC becomes bistable in the model, and if the AMOC collapses, this could be irreversible.

Here, we use the 450 ppm simulation as a representative example (which corresponds to the global equilibrium at 2.1 °C warming, see also Supplementary Fig. 4a) to illustrate the detailed evolution of temperature response during the hosing experiment. In our results, during the hosing period, the AMOC weakens until collapse (Fig. 1b–d), displaying AMOC streamfunction variations that are consistent with other Earth System Model simulations²⁰. To investigate the impact of AMOC collapse, we only focus on a hosing rate of 0.2 Sv in the subsequent analysis, which ensures that all cases eventually lead to collapse.

Climate response to AMOC collapse

We investigate the long-term regional temperature responses to an AMOC collapse. The fully coupled model simulations show that, after reaching a re-established equilibrium following an AMOC collapse, the climate exhibits a strongly asymmetric hemispheric temperature response: pronounced cooling in the Northern Hemisphere and concurrent warming in the Southern Hemisphere, reflecting a global redistribution of heat (Fig. 2c). All three model setups show similar spatial response patterns (Supplementary Fig. 6). The Northern Hemisphere cooling simulated here, consistent across all CO₂ baselines (Fig. 2d, f), aligns with previous modeling studies collapsing the AMOC under pre-industrial conditions^{20,38,39,53}. However, our simulations exhibit a much more pronounced warming in the Southern Hemisphere across all CO₂ baselines than in pre-industrial cases in previous studies (Fig. 2c). In this scenario, the Arctic regions (60 °N – 90 °N) cool by around 7 °C after the AMOC collapse (Fig. 2d), and the North Atlantic cooling is stronger than in other regions at comparable latitudes. AMOC collapse leads to a sharp reduction in the transport of heat to northern North Atlantic, which causes cooling strongly amplified by sea-ice-albedo feedback^{20,54}. The cooling of the Arctic leads to a considerable increase in Arctic sea ice area, leading to an increase in albedo (Supplementary Fig. 7), which further causes cooling in the Northern Hemisphere. Cooling occurs in the Northern Hemisphere, intensifying over regions north of 60 °N,

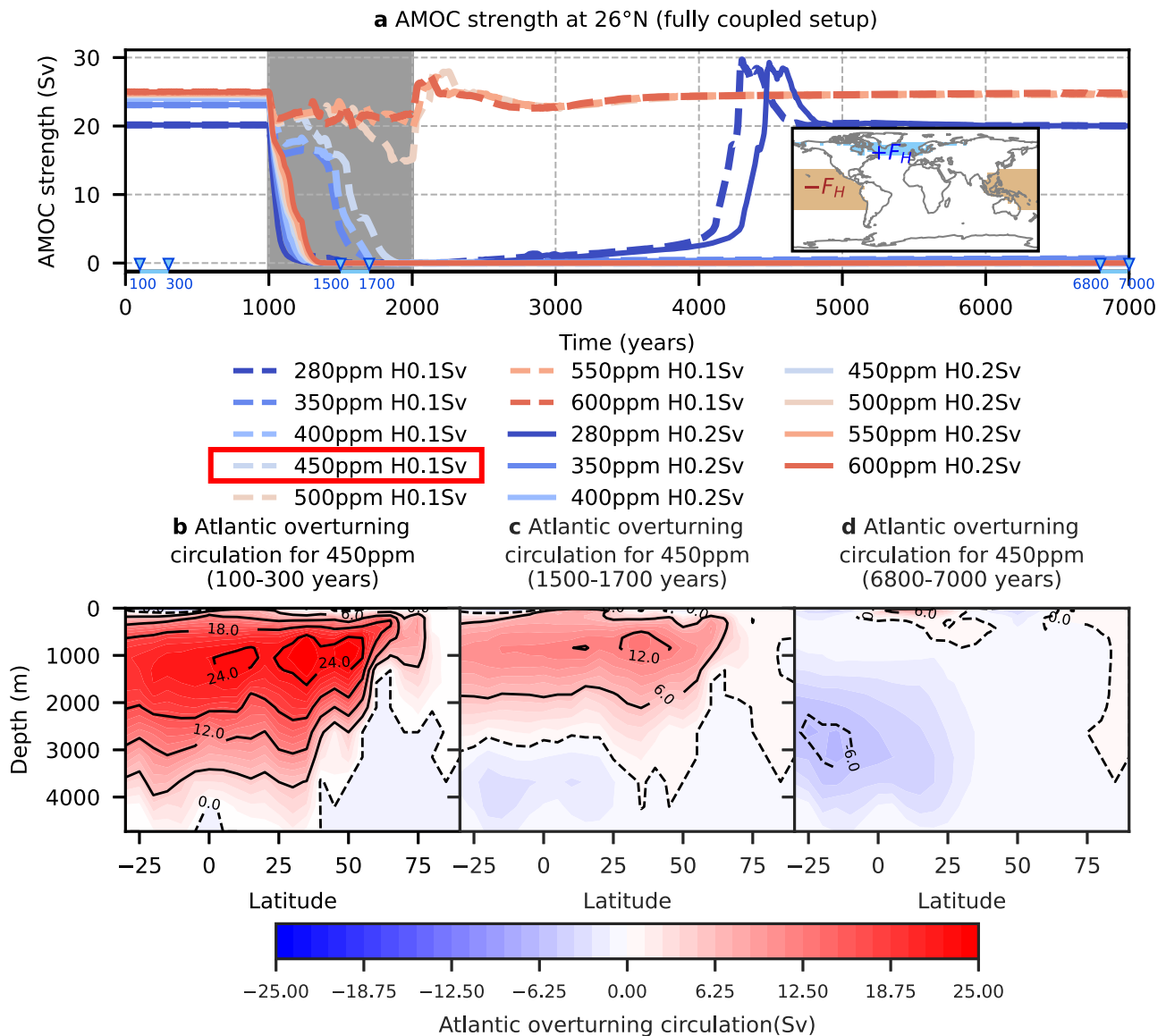


Fig. 1 | AMOC response to freshwater hosing from an equilibrium state under different baseline CO₂ levels in fully coupled model setup. a AMOC strength (maximum Atlantic overturning circulation) at 26°N, where the gray shading indicates the period with freshwater hosing. The dashed lines represent a hosing strength of 0.1 Sv, while the solid lines correspond to a hosing strength of 0.2 Sv.

Inset: In the hosing experiment, freshwater is added to the Atlantic Ocean surface between 50°N and 70°N (+F_H) and compensated in the Pacific between 30°S and 30°N (-F_H). The streamfunction of the AMOC at 450 ppm before, during and after collapse for the 0.1 Sv-hosing experiment is shown in (b-d), averaged over model years 100–300 (b), 1500–1700 (c), 6800–7000 (d).

which is similar to the pattern of temperature changes after the collapse of the AMOC in some simulations under pre-industrial^{10,20,39}. In contrast, the Antarctic regions (60°S – 90°S) warm by around 6 °C (Fig. 2f). Because our simulations do not include ice sheet modules, the result does not account for the additional effect resulting from melting ice sheets (e.g., those in Antarctica and Greenland). The magnitude of the long-term regional temperature changes induced by AMOC collapse is broadly similar across the different experiments of CO₂ baselines (Fig. 2d, f). The spatial pattern is also similar, with persistent North Atlantic cooling in all cases. When the background greenhouse warming associated with a 450ppm baseline (Fig. 2a) is superimposed on the AMOC collapse response, the overall climate state (relative to pre industrial conditions) features intense warming in the Antarctic and pronounced cooling in the North Atlantic (Fig. 2e). Therefore, in some regions south of 60°S, the combined warming effect may exceed 10 °C. The cooling is reduced over the Northern Hemisphere, where greenhouse warming partially offsets the temperature decline induced by the AMOC collapse.

On a global scale, our results indicate that the AMOC collapse leads to a net increase in GMT (Fig. 2b), indicating an additional warming effect globally. If the AMOC stabilizes in an off state after the collapse, global temperatures eventually stabilize at 0.17–0.27 °C higher than before water hosing, across the different CO₂ baselines (Fig. 3d). The transition from AMOC weakening to collapse is accompanied by characteristic temperature changes. After the start of hosing, the GMT first drops rapidly under the baseline GMT and ΔGMT_{AMOC} remains below -0.5 °C during the AMOC's weakening and transition, then rebounds above the pre-hosing baseline temperature. (Fig. 3b and Fig. 2a). This closely aligns with the findings of Boot et al. (2024)⁴², where the AMOC collapse induces strong cooling around the transition point, with temperatures changing by approximately -1 °C before gradually recovering.

Having established a net additional warming following the AMOC collapse, we next examine results from different model setups to explore the mechanisms driving this response. We first assess the climate response to AMOC collapse under fixed-CO₂ model setup, i.e. excluding the carbon

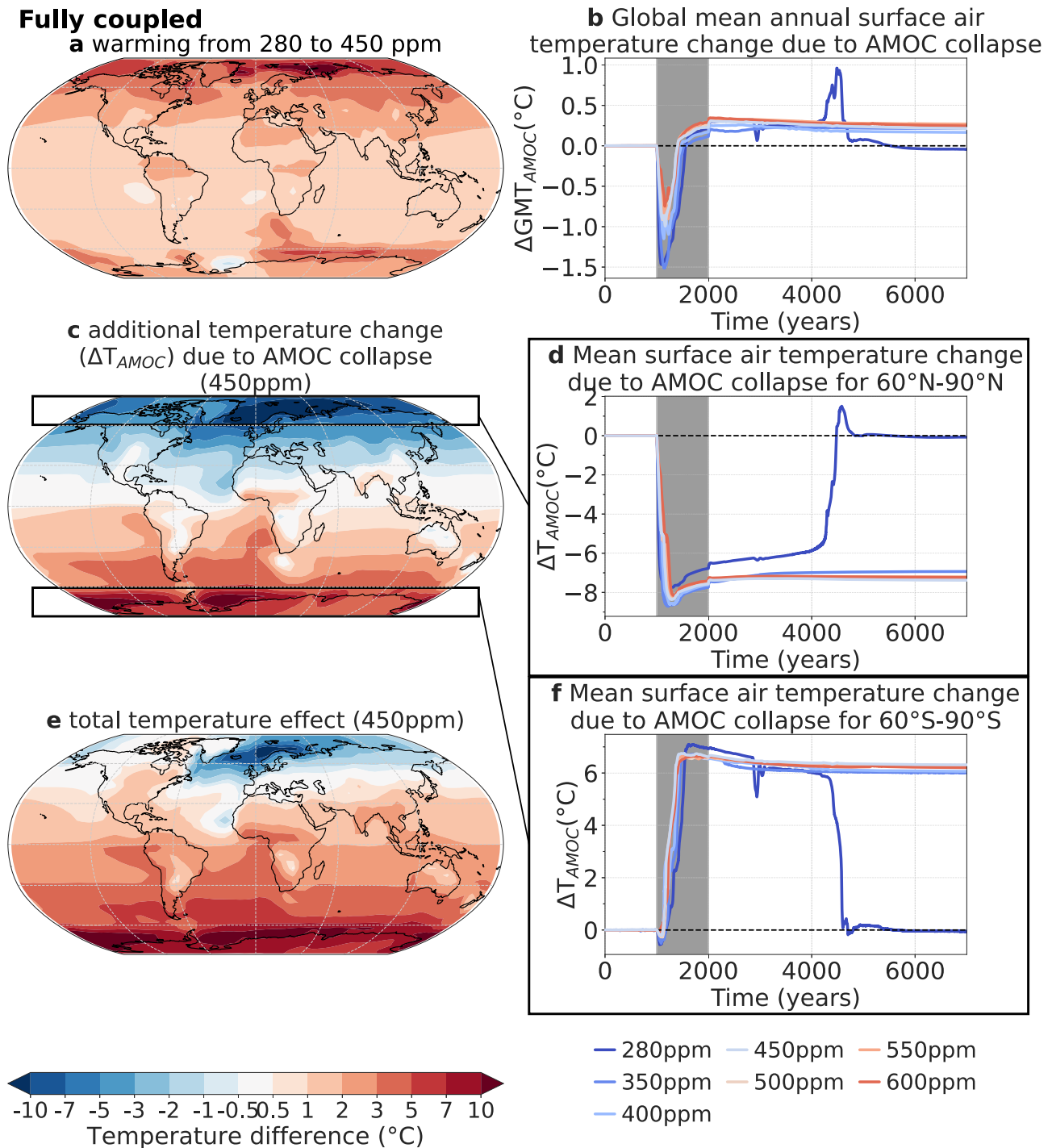
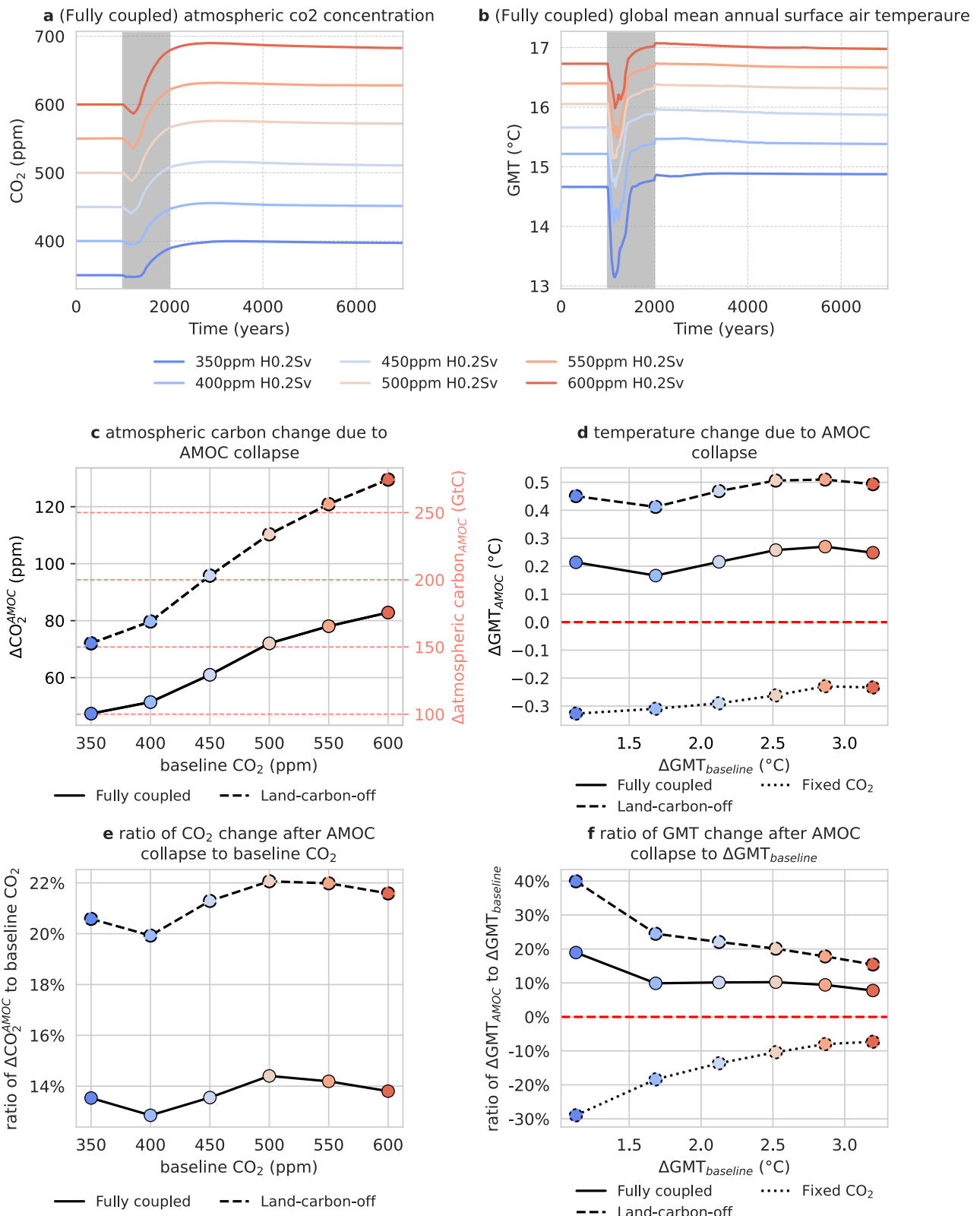


Fig. 2 | Changes in surface air temperature due to AMOC collapse for the fully coupled model setup in the experiments with a hosing rate of 0.2 Sv. a Spatial distribution of temperature difference resulting from baseline CO₂ level (450 ppm) above pre-industrial condition, calculated as the temperature difference between the baseline equilibrium state and the pre-industrial temperature. **c** Temperature change due to AMOC collapse at 450 ppm (ΔT_{AMOC}), determined by subtracting the baseline equilibrium temperatures from the final state after AMOC collapse. **e** Total temperature response to the AMOC collapse at 450 ppm baseline experiment,

calculated as the difference between the final equilibrium state after AMOC collapse and the pre-industrial state. Changes in mean surface air temperature due to AMOC collapse for the full coupled model setup under various baseline CO₂ levels during hosing experiments (computed as the difference from each experiment's initial value): **(b)** global mean surface air temperature anomaly (ΔGMT_{AMOC}), **(d)** mean surface temperature change over 60°N – 90° N, and **(f)** mean surface temperature change over 60°S – 90°S.

cycle effects. In this model setup, both land and ocean carbon cycles are disabled and CO₂ remains constant over time. Comparing the equilibrium GMT after the AMOC collapse with that before the freshwater hosing input shows a global mean temperature decrease of 0.2 to 0.3 °C (Fig. 3d). This suggests that oceanic physical processes associated with the AMOC collapse

exert a cooling influence on the global climate. We then examine the roles of the ocean and land carbon cycles. When the land carbon response is disabled (land-carbon-off setup), the GMT increases by 0.41–0.51 °C after the AMOC collapse (Fig. 3d). Compared with the fixed-CO₂ setup, where physical ocean processes alone induce global cooling, this warming response



indicates that changes in the ocean carbon cycle contribute to a net additional warming. The stronger GMT increase in the land-carbon-off model setup relative to the full coupled setup further suggests that the land carbon cycle exerts a compensating cooling effect. Overall, the net additional warming in the fully coupled model is primarily driven by changes in the ocean carbon cycle during the AMOC collapse (Fig. 3a).

Carbon cycle response after AMOC collapse

We next examine how the atmospheric CO₂ concentration changes over time after the end of the hosing experiment towards equilibrium in the simulations with interactive CO₂. The results indicate that both the fully coupled and land-carbon-off model setups show a rise in atmospheric CO₂ concentration as the AMOC begins to weaken, across all baseline CO₂ levels

Fig. 3 | Changes in atmospheric CO₂ and global mean annual surface air temperature (GMT) after AMOC collapse down under various baseline CO₂ levels. (a, b) display the atmospheric CO₂ concentration and GMT response to freshwater hosing over time in the fully coupled model setup. (c) Illustrates the difference in atmospheric CO₂ concentrations between equilibrium states before and after AMOC collapse ($\Delta\text{CO}_2^{\text{AMOC}}$) for the fully coupled and land-carbon-off model setups. $\Delta\text{CO}_2^{\text{AMOC}}$ is computed using the average over the final 500 years (6500–7000) minus the average over the first 500 years (0–500) of the simulation under each CO₂ baseline. e Presents the corresponding ratio of $\Delta\text{CO}_2^{\text{AMOC}}$ relative to the baseline CO₂ (pre-hosing atmospheric CO₂ levels) for both the fully coupled and land-carbon-off

model setups. In the fixed CO₂ model setup, atmospheric CO₂ concentrations remain constant throughout the entire simulation. d Illustrates the additional GMT changes due to AMOC collapse ($\Delta\text{GMT}_{\text{AMOC}}$) as a function of $\Delta\text{GMT}_{\text{baseline}}$, where $\Delta\text{GMT}_{\text{baseline}}$ represents the difference between the initial GMT under each baseline CO₂ level and the pre-industrial GMT. Specifically, $\Delta\text{GMT}_{\text{baseline}}$ is calculated using the first 500-year average GMT under each baseline CO₂ level minus the first 500-year average pre-industrial GMT (Supplementary Fig. 4a). Panel (f) presents the ratio of $\Delta\text{GMT}_{\text{AMOC}}$ to $\Delta\text{GMT}_{\text{baseline}}$ for the fully coupled, land-carbon-off, and fixed-CO₂ model setups. All results in are based on experiments utilizing 0.2 Sv hosing to assess responses following AMOC collapse.

(Fig. 3a). In the fully coupled version, the irreversible collapse of the AMOC would lead to an increase in atmospheric CO₂ concentration by 47–83 ppm (100GtC to 175GtC in atmospheric carbon inventory) across the 6 experiments conducted under the baseline CO₂ levels from 350 ppm to 600 ppm, with larger increases occurring at higher baseline CO₂ levels. Under the 280-ppm baseline, our simulated CO₂ rise during AMOC collapse (~30 ppm; Supplementary Fig. 2) falls within the upper range of previous estimates³⁷, whereas higher-CO₂-baseline cases in our study yield much stronger releases. In the land-carbon-off setup, where the terrestrial carbon cycle is disabled, AMOC collapse leads to an even larger CO₂ increase, by 72–130 ppm (153GtC to 275GtC in atmospheric carbon inventory), as the compensating land carbon sink is absent (Fig. 3c). In contrast, in the fully coupled setup, the land carbon cycle functions as a carbon sink (Supplementary Fig. 8), absorbing part of the carbon released from the ocean following the AMOC shutdown. In all three model setups, carbon exchanges occur only among the ocean, land and atmosphere, with no exchange with geological reservoirs; hence, in the land-carbon-off setup, atmospheric CO₂ increases entirely from oceanic release. Moreover, while the additional atmospheric CO₂ concentration change increases linearly with the baseline background CO₂ level, the ratio of this increase to the baseline CO₂ level remains consistently around 20% to 22% for land-carbon-off setup, while the ratio is lower for the fully coupled setup at around 13% (Fig. 3e), illustrating the compensating effect of the terrestrial carbon sink (Supplementary Fig. 8). Our findings thus indicate that an AMOC collapse could substantially increase atmospheric CO₂ concentrations.

Overall, our results indicate ocean dynamics induce global cooling, while ocean carbon release increases atmospheric CO₂ resulting in a net global warming of about 0.2 °C in the fully coupled model setup (Fig. 3d), even though the land carbon sink offsets some of the CO₂-induced warming. We compare the ratio of additional GMT change from AMOC collapse to the GMT increase due to baseline CO₂ rise from the preindustrial level. In the fully coupled version, as baseline CO₂ levels increase from 350 ppm to 600 ppm, this ratio drops from ~19% to ~8% (Fig. 3f), indicating that AMOC collapse contributes relatively less to GMT change at higher CO₂ levels. This implies that the relative temperature response triggered by AMOC collapse is stronger and more detrimental at lower CO₂ levels.

Southern Ocean convection following AMOC shutdown

As the AMOC collapse is accompanied by substantial oceanic CO₂ outgassing, resulting in additional warming, we investigate associated ocean circulation changes and find that deep Southern Ocean convection plays a key role in driving this ocean carbon release. With the start of hosing, the AMOC weakens rapidly, reducing North Atlantic circulation depth (Fig. 1b–d and Supplementary Fig. 9a, b) while enhancing deep convection over the Southern Ocean (Fig. 4f–h and Supplementary Fig. 9a, b). CLIMBER-X has previously been shown to reproduce the main large-scale features of the present-day global air–sea CO₂ flux pattern⁴⁶, including a carbon source in the eastern equatorial Pacific and a pronounced sink in the North Atlantic, broadly consistent with observational estimates^{55–57}. In our study, under warmer equilibrium climates with higher CO₂ baseline conditions, the Southern Ocean exhibits a stronger carbon source than in pre-industrial run (280 ppm). Changes in global overturning circulation after AMOC collapse redistribute global ocean carbon sink and source patterns

(Fig. 4). Both the carbon sink and source in the North Atlantic region weaken and the carbon sink distributed in the Northern Hemisphere shifts southward overall after AMOC collapse (Supplementary Fig. 10a). The mixed layer depth in the 70 °S–80 °S region deepens rapidly around the AMOC transition (Supplementary Fig. 10b–e), indicating the formation of deep convection in the Southern Ocean (Fig. 4g). This convection coincides with enhanced Southern oceanic CO₂ flux to the atmosphere across the same latitude band (Supplementary Fig. 10a). As a result, the deep ocean is strongly ventilated (as indicated by the water-age tracer in Supplementary Fig. 10f–h), leading to a release of carbon in the Southern Ocean around Antarctica, which dominates the global oceanic CO₂ outgassing (Supplementary Fig. 9f), and a large increase in atmospheric CO₂. The deep water formation also keeps large parts of the Southern Ocean ice-free, resulting in a pronounced warming over the region (Supplementary Fig. 7). Overall, both the large increase in carbon flux from ocean to atmosphere and warming in the Southern Hemisphere in response to an AMOC collapse in our simulations are a consequence of widespread deep convection being eventually triggered in the Southern Ocean (Supplementary Fig. 10).

Support for this model response in the Southern Ocean comes from CO₂ changes during Heinrich events observed in paleoclimate records. Large iceberg discharges from the Laurentide ice sheet during the last glacial period led to an AMOC collapse and proxy records from Antarctic ice cores show a large and abrupt increase of both Antarctic temperature and atmospheric CO₂ some centuries after the AMOC shutdown, which have been suggested to be related to a possible start of convection around Antarctica at that time^{58,59}. CLIMBER-X has recently been shown to realistically reproduce these features as a response to an AMOC collapse produced by the addition of freshwater flux in the North Atlantic to mimic a Heinrich event⁶⁰. In that study, it was also shown that the start of convection in the Southern Ocean as a response to an AMOC collapse is a robust feature of the model. The mechanisms behind this so-called bipolar convection seesaw are described in detail in ref. 60 and basically involve a destratification of the Southern Ocean in response to an AMOC shutdown, which eventually leads to convective instability around Antarctica. As shown in this paper, this is not just a feature of cold climates, but could plausibly also occur in response to a future AMOC collapse (Supplementary Fig. 7 and Supplementary Fig. 10). It is this model feature that produces the exceptionally large CO₂ response responsible for the overall global warming effect of an AMOC shutdown.

Discussion

Our CLIMBER-X simulations reveal the impact of AMOC collapse on ocean carbon storage and its effect on long-term global climate under different CO₂ levels, ranging from pre-industrial levels (280 ppm) to more than doubling of pre-industrial CO₂ concentration (600 ppm). These results highlight the role of the AMOC as a key regulator of global climate. The CO₂ rise associated with AMOC collapse causes an additional global warming of about 0.2 °C. The substantial regional temperature responses, however, originate primarily from the direct physical effects of AMOC collapse on climate. Our results show that, at the equilibrium climate across all baseline CO₂ levels, the AMOC collapse would lead to pronounced regional responses: a cooling by around 7 °C over the Arctic (60 °N – 90 °N) and a warming by around 6 °C over the Antarctic (60 °S – 90 °S) (Fig. 2). An

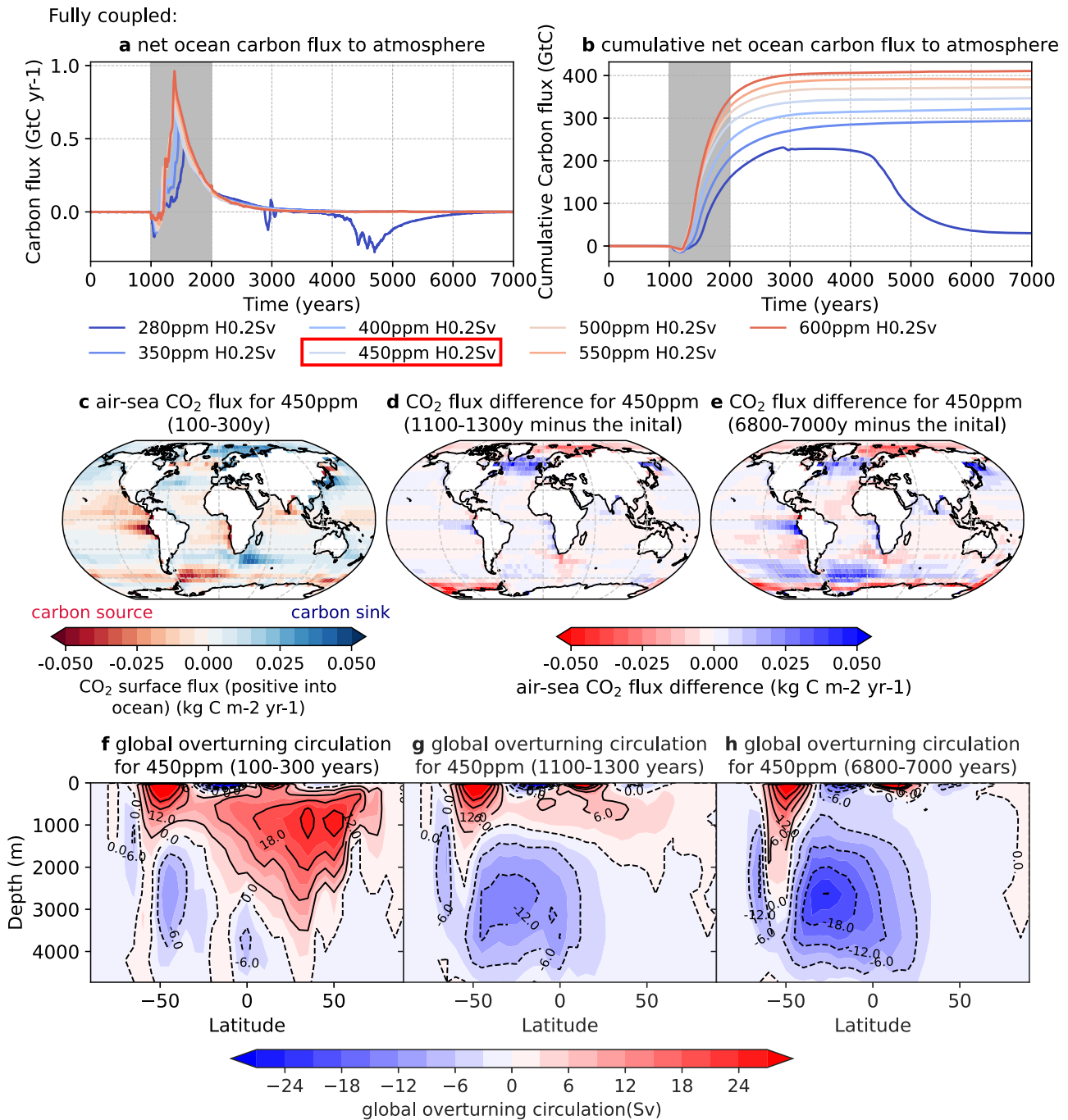


Fig. 4 | The ocean carbon flux and global overturning circulation before and after AMOC collapse for fully coupled version with a hosing rate of 0.2 Sv. During the process, the changes of net and cumulative ocean carbon flux to the atmosphere under different CO₂ levels are shown in (a, b), respectively. The initial global air-sea CO₂ flux patterns at 450 ppm is shown in (c), averaged over model year 100–300. (d, e) show the difference in air-sea CO₂ flux between the average and the initial for

model years 1100–1300 and 6800–7000, respectively. The positive values of CO₂ flux indicate carbon flux into the ocean and negative values represent carbon release from the ocean. The streamfunctions of global overturning circulations before and after the AMOC collapse under 450 ppm, averaged over model years 100–300 (f), 1100–1300 (g), 6800–7000 (h) are illustrated respectively.

AMOC collapse may cause the release of large amounts of carbon stored in the Southern Ocean to the atmosphere. While ocean dynamics during AMOC shutdown induce global cooling in the fixed-CO₂ setup, the substantial ocean carbon release in the fully coupled setup increases atmospheric CO₂ levels, and even with considerable land carbon uptake, the remaining CO₂ offsets the cooling and contributes to additional warming. Our results indicate that under equilibrium warmer climate conditions with 350 ppm to 600 ppm of CO₂, an AMOC collapse may release enough carbon

to cause a CO₂ increase by 47–83 ppm. Most of this CO₂ rise is the result of convection being triggered in the Southern Ocean as a response to the forced AMOC shutdown.

Our results show that AMOC collapse induces much stronger CO₂ increases at higher baseline CO₂ levels (compared to 280 ppm), which is further supported by paleoclimate evidence. Recent studies show that CLIMBER-X reproduces critical aspects of millennial-scale climate variability during glacial times⁶¹. In particular, consistent with more complex

models (e.g., Vettoretti et al. 2022⁶²; Malmierca-Vallett et al. 2024⁶³), it produces Dansgaard-Oeschger like events as part of internal variability of the climate system under mid-glacial ice sheets and low CO₂⁶¹. It is widely accepted that these Dansgaard-Oeschger events are associated with abrupt changes in the AMOC, involving transitions between weak and strong AMOC states. However, Dansgaard-Oeschger variability is not associated with a complete collapse of the AMOC and ice core data show only minor responses of atmospheric CO₂ of ~ 5 ppm during Dansgaard-Oeschger events⁶⁴. This is consistent with what was found in model simulations (e.g., see ref. 65) and also with what CLIMBER-X produces⁶⁰. As a response to a complete AMOC shutdown following freshwater input into the North Atlantic from Heinrich events during glacial times, CLIMBER-X produces a much larger response in atmospheric CO₂ of ~ 15 ppm, which is again in good agreement with ice core data during Heinrich Stadials⁶⁰. The process behind this large CO₂ increase is a sudden onset of convection in the Southern Ocean in response to an AMOC shutdown⁶⁰. Several studies have suggested that deep Southern Ocean convection can promote the release of stored oceanic carbon^{37,66,67}. Because CLIMBER-X reproduces past climate-carbon cycle variability linked to AMOC changes, we have confidence in its response to a potential AMOC collapse under warmer conditions. In our simulations, the comparatively larger atmospheric CO₂ increase is primarily associated with the development of deep Southern Ocean convection, which ventilates carbon-rich deep waters and drives substantial outgassing to the atmosphere. The CO₂ increase in response to an AMOC shutdown grows strongly with higher baseline CO₂ levels (Fig. 3c). Higher CO₂ baselines correspond to larger ocean carbon inventories (Supplementary Fig. 11), contributing to substantially more carbon to be released during a collapse, suggesting that the amplitude of past glacial CO₂ responses is not a proper analog for the expected amplitude of CO₂ increase in a warmer, higher-CO₂ world. Consistent with this, other models show that in warmer climates a sudden Southern ocean convection onset can raise atmospheric CO₂ by ~ 40 ppm⁶⁶, much larger than observed glacial-period changes. Our results suggest that the same Southern Ocean convection-driven mechanism could operate under future warmer conditions, producing a substantially larger CO₂ response than during glacial times.

It is important to emphasize that our study focuses on the long-term climate response to the AMOC collapse induced by freshwater hosing in an equilibrium climate, which differs from studies of the transient climate change driven by CO₂ emission scenarios (e.g., see refs. 42,68). Distinguishing responses to AMOC behavior under transient versus equilibrium background conditions is crucial: in CLIMBER-X, the AMOC weakens during transient warming, consistent with CMIP models⁴², but subsequently recovers and stabilizes in a stronger equilibrium state for baseline CO₂ concentrations of 350–600 ppm (Supplementary Fig. 1). To isolate the AMOC effect in these warmer background climates, we therefore performed all hosing experiments under equilibrium conditions (280–600 ppm). In this case, higher CO₂ baseline equilibrium states correspond to greater initial AMOC strength (Supplementary Fig. 1 and Supplementary Fig. 4b) and resilience, as evidenced by the stronger freshwater forcing required to trigger collapse (Fig. 1a). This suggests that our findings are conservative, in the sense that AMOC collapse with subsequent net-warming outcomes, occurs even with a stronger AMOC at the outset.

We focus on the integrated carbon response following AMOC collapse without decomposing individual mechanisms (e.g., solubility or biological pump effects⁶⁹) in this study. Intermodel differences in AMOC sensitivity⁷⁰, together with known biases in North Atlantic deep-water formation⁷¹, salinity, and meltwater runoff⁷², and background climatological states³⁷ may influence the magnitude and thresholds of carbon responses to AMOC collapse across models. However, our results indicate that these factors play a secondary role compared with the dominant ventilation-driven carbon loss (Supplementary Fig. 9c–f). The total ocean carbon declines almost entirely through reduced dissolved inorganic carbon, and the dissolved inorganic carbon loss closely matches the cumulative ocean-to-atmosphere carbon flux (Supplementary Fig. 9c, d). Changes in dissolved and particulate

organic carbon are comparatively minor (There is a difference in magnitude) (Supplementary Fig. 9e). As the system re-equilibrates after the collapse, the global mean net air–sea CO₂ flux stabilizes near zero, whereas the sharp release during the collapse corresponds to pronounced Southern Ocean outgassing. In contrast, surface carbon flux changes in the Pacific and Indian Oceans are minor, while the Atlantic evolves from a temporary enhancement of the sink at the onset to a weakened and eventually nearly neutral state (Supplementary Fig. 9f). These surface carbon flux evolutions over different oceans explain the changes in atmospheric CO₂. The sharp transient outgassing in our simulations is driven by deep Southern Ocean convection that ventilates carbon-rich waters.

Our experiments show that terrestrial carbon sinks may partially mitigate the impact of oceanic carbon release triggered by AMOC collapse and the induced deep convection in the Southern Ocean (Supplementary Fig. 8). Although the impacts on the terrestrial carbon cycle are not the main focus of this study, they are still important. Our results show that the absorption of carbon by the land markedly reduces the additional global mean warming from 0.41–0.51 °C to around 0.17–0.27 °C (Fig. 3). However, several model studies indicate that an AMOC collapse may lead to substantial terrestrial carbon loss, increasing atmospheric CO₂ by up to ~ 20 ppm, primarily due to tropical drying and reduced vegetation productivity^{73–75}. At present, human land-use change has already converted large terrestrial carbon sources such as the Amazon rainforest from a carbon sink to a carbon source^{76,77}. This means that while terrestrial carbon sinks remain important for global climate stability, their future evolution is uncertain and will depend on complex interactions between climate change and human land use.

In this study, the prescribed freshwater perturbations (0.1 and 0.2 Sv) are used as idealized hosing experiments to demonstrate AMOC bistability under different background CO₂ levels and to evaluate the subsequent Earth system response, rather than to represent specific real-world forcing scenarios. Under high-emission scenarios, a near-complete loss of the Greenland Ice Sheet could generate roughly 0.1 Sv of freshwater input (0.1 Sv = 10⁶ m³ s⁻¹ ≈ 3, 156 Gt yr⁻¹)⁷⁸. Thus, our idealized forcings fall within a plausible envelope for testing AMOC sensitivity. Finally, the model does not include dynamic ice sheets, so Antarctic meltwater and its teleconnections are not represented. Recent work shows that West Antarctic meltwater release can affect AMOC resilience⁷⁹, and incorporating Antarctic meltwater effects remains an important avenue for future work.

In summary, this study comprehensively analyzed the possible impacts of AMOC collapse on the ocean carbon cycle and climate response under a series of CO₂ baseline equilibria. The results emphasize that under the various climate warming equilibrium, the potential collapse of AMOC may lead to substantial ocean carbon release to the atmosphere, leading to additional global warming and producing pronounced regional responses. Although such long-term equilibrium responses may not be fully realized in the real world, they provide valuable insight into the underlying physical mechanisms and potential climate and ocean carbon responses. Importantly, while the additional global warming is modest, the substantial regional temperature responses, such as multi-degree warming over parts of Antarctica under a 450-ppm background, highlight the substantial climate risks associated with an AMOC collapse.

Methods

CLIMBER-X is a fast Earth system model⁴⁵ that includes a 3D frictional-geostrophic ocean model GOLDSTEIN with 23 vertical layers⁸⁰, a semi-empirical statistical dynamical atmosphere model SESAM⁴⁵, a sea ice model SISIM⁴⁵, and a land surface model PALADYN with dynamic vegetation⁸¹, which can simulate the global carbon cycle in Earth systems⁴⁵. CLIMBER-X's simulation performance of the Earth system under different forcing and boundary conditions is comparable to that of the most advanced CMIP6 models, especially the simulation performance of the current AMOC profile fits the CMIP6 model and climate observations well⁴⁵. Moreover, CLIMBER-X also shows its ability to simulate the multi-stability of the AMOC system under different boundary conditions^{43,61}.

To simulate the collapse of the AMOC and further analyze its impact on the global carbon cycle and global temperature, we use CLIMBER-X in a climate-carbon cycle set up including atmosphere, ocean, land with dynamic vegetation and carbon cycle, sea ice and ocean biogeochemistry. We do not use the ice sheet model and this paper does not involve the study of ice sheet changes. To further analyze the role of ocean activity and carbon cycle in the AMOC shutdown process, we designed experiments to quantify the role of each component by setting: (1) a fully coupled system (Fully coupled), which includes all the above modules, (2) a version in which the land carbon cycle is disabled, leaving only the ocean carbon cycle to interact with the atmosphere (land-carbon-off) with the influence of vegetation and soil carbon cycle processes being ignored and 3) a fixed-CO₂ setup to estimate the pure climate response to the AMOC shutdown (Fixed-CO₂) in which CO₂ remains constant at the baseline CO₂ level throughout the entire process and the temperature response comes entirely from ocean, atmosphere and land dynamics, among which the sea ice-albedo feedback is dominant.

A 10,000-year spinup run is first performed under each CO₂ baseline to ensure the system reaches equilibrium (Supplementary Fig. 1). Subsequently, a 7000-year experiment is conducted for each equilibrated state, with freshwater hosing applied during model years 1000–2000. Freshwater hosing is performed at strengths of 0.1 Sv and 0.2 Sv in the North Atlantic in the range of 50 °N–70 °N. In our experiments, freshwater hosing of 0.1 Sv proved insufficient to induce AMOC collapse under atmospheric CO₂ concentrations of 550 ppm and 600 ppm; consequently, the freshwater flux was increased to 0.2 Sv to ensure consistent AMOC collapse across all experimental scenarios. To keep global salinity constant, a compensating flux of the same magnitude and opposite sign was applied in the Pacific between 20 °N and 50 °N. We tested global compensation of the freshwater flux, instead of only in the tropical Pacific, and found little impact on the results. After the end of the hosing the run is continued until model year 7000 to ensure that the system returns to equilibrium. We investigate the carbon cycle and climate responses across various climate conditions by conducting the same spinup and freshwater hosing experiment under CO₂ concentrations ranging from pre-industrial (280 ppm) to 600 ppm.

Data availability

All datasets analyzed in this study, generated using the CLIMBER-X model, are available at <https://doi.org/10.5281/zenodo.15277288>. This repository also includes the code used to create all the figures presented in the manuscript.

Code availability

The CLIMBER-X model is freely available as open-source code at <https://github.com/cxesmc/climber-x>, last access: 3 Feb 2026. For this study we used v1.3.0 of the model.

Received: 10 February 2025; Accepted: 11 March 2026;

Published online: 27 March 2026

References

- Kirchengast, G. & Pichler, M. A traceable global warming record and clarity for the 1.5 °C and well-below-2 °C goals. *Commun. Earth Environ.* **6**, 402 (2025).
- Cannon, A. J. Twelve months at 1.5 c signals earlier than expected breach of paris agreement threshold. *Nat. Clim. Change* **15**, 266–269 (2025).
- Bevacqua, E., Schleussner, C.-F. & Zscheischler, J. A year above 1.5 °C signals that earth is most probably within the 20-year period that will reach the Paris agreement limit. *Nat. Clim. Change* **15**, 262–265 (2025).
- Rockström, J. et al. A roadmap for rapid decarbonization. *Science* **355**, 1269–1271 (2017).
- Wolosin, M. Exponential roadmap for natural climate solutions <https://www.conservation.org/priorities/exponential-roadmap-natural-climate-solutions>. Accessed: 2024-08-27 (2022).
- DeVries, T. The ocean carbon cycle. *Annu. Rev. Environ. Resour.* **47**, 317–341 (2022).
- Friedlingstein, P. et al. Global carbon budget 2023. *Earth Syst. Sci. Data* **15**, 5301–5369 (2023).
- Masson-Delmotte, V. et al. (eds.) *IPCC, 2021: Summary for Policymakers. In: Climate Change 2021: The Physical Science Basis* (Cambridge University Press, Cambridge, UK and New York, NY, USA, 2023).
- Brown, P. J. et al. Circulation-driven variability of Atlantic anthropogenic carbon transports and uptake. *Nat. Geosci.* **14**, 571–577 (2021).
- Armstrong McKay, D. I. et al. Exceeding 1.5 °C global warming could trigger multiple climate tipping points. *Science* **377**, eabn7950 (2022).
- Stommel, H. Thermohaline convection with two stable regimes of flow. *Tellus* **13**, 224–230 (1961).
- Manabe, S. & Stouffer, R. J. Two stable equilibria of a coupled ocean-atmosphere model. *J. Clim.* **1**, 841–866 (1988).
- Stocker, T. F. & Wright, D. G. Rapid transitions of the ocean’s deep circulation induced by changes in surface water fluxes. *Nature* **351**, 729–732 (1991).
- Rahmstorf, S. Bifurcations of the Atlantic thermohaline circulation in response to changes in the hydrological cycle. *Nature* **378**, 145–149 (1995).
- Rahmstorf, S. et al. Thermohaline circulation hysteresis: A model intercomparison. *Geophys. Res. Lett.* **32**, L23605 (2005).
- van Westen, R. M. & Dijkstra, H. A. Asymmetry of amoc hysteresis in a state-of-the-art global climate model. *Geophys. Res. Lett.* **50**, e2023GL106088 (2023).
- Stouffer, R. J. et al. Investigating the causes of the response of the thermohaline circulation to past and future climate changes. *J. Clim.* **19**, 1365–1387 (2006).
- Jackson, L. et al. Global and European climate impacts of a slowdown of the AMOC in a high resolution GCM. *Clim. Dyn.* **45**, 3299–3316 (2015).
- Bonnet, R. et al. Increased risk of near term global warming due to a recent AMOC weakening. *Nat. Commun.* **12**, 6108 (2021).
- van Westen, R. M., Kliphuis, M. & Dijkstra, H. A. Physics-based early warning signal shows that AMOC is on tipping course. *Sci. Adv.* **10**, eadk1189 (2024).
- Ben-Yami, M. et al. Impacts of AMOC collapse on monsoon rainfall: A multi-model comparison. *Earth’s Future* **12**, e2023EF003959 (2024).
- Ganopolski, A. & Rahmstorf, S. Rapid changes of glacial climate simulated in a coupled climate model. *Nature* **409**, 153–158 (2001).
- Henry, L. et al. North Atlantic ocean circulation and abrupt climate change during the last glaciation. *Science* **353**, 470–474 (2016).
- Menviel, L. C., Skinner, L. C., Tarasov, L. & Tzedakis, P. C. An ice-climate oscillatory framework for Dansgaard-Oeschger cycles. *Nat. Rev. Earth Environ.* **1**, 677–693 (2020).
- Manabe, S. & Stouffer, R. J. Century-scale effects of increased atmospheric CO₂ on the ocean-atmosphere system. *Nature* **364**, 215–218 (1993).
- Gregory, J. et al. A model intercomparison of changes in the Atlantic thermohaline circulation in response to increasing atmospheric CO₂ concentration. *Geophys. Res. Lett.* **32**, L12703 (2005).
- Bonan, D. B., Thompson, A. F., Newsom, E. R., Sun, S. & Rugenstein, M. Transient and equilibrium responses of the Atlantic Overturning Circulation to warming in coupled climate models: The role of temperature and salinity. *J. Clim.* **35**, 5173–5193 (2022).
- Romanou, A. et al. Stochastic bifurcation of the North Atlantic circulation under a midrange future climate scenario with the NASA-GISS model. *J. Clim.* **36**, 6141–6161 (2023).

29. Moat, B. I. et al. Pending recovery in the strength of the meridional overturning circulation at 26 n. *Ocean Sci.* **16**, 863–874 (2020).
30. Caesar, L., McCarthy, G., Thornalley, D., Cahill, N. & Rahmstorf, S. Current Atlantic Meridional Overturning Circulation weakest in last millennium. *Nat. Geosci.* **14**, 118–120 (2021).
31. Latif, M., Sun, J., Visbeck, M. & Hadi Bordbar, M. Natural variability has dominated Atlantic Meridional Overturning Circulation since 1900. *Nat. Clim. Change* **12**, 455–460 (2022).
32. Masson-Delmotte, V. et al. (eds.) *IPCC, 2021: Technical Summary. In Climate Change 2021: The Physical Science Basis.* (Cambridge University Press, Cambridge, UK and New York, NY, USA, 2023).
33. Boers, N. Observation-based early-warning signals for a collapse of the Atlantic Meridional Overturning Circulation. *Nat. Clim. Change* **11**, 680–688 (2021).
34. Ditlevsen, P. & Ditlevsen, S. Warning of a forthcoming collapse of the Atlantic Meridional Overturning Circulation. *Nat. Commun.* **14**, 1–12 (2023).
35. Sarmiento, J. L. & Le Quere, C. Oceanic carbon dioxide uptake in a model of century-scale global warming. *Science* **274**, 1346–1350 (1996).
36. Schmittner, A. & Galbraith, E. D. Glacial greenhouse-gas fluctuations controlled by ocean circulation changes. *Nature* **456**, 373–376 (2008).
37. Gottschalk, J. et al. Mechanisms of millennial-scale atmospheric CO₂ change in numerical model simulations. *Quat. Sci. Rev.* **220**, 30–74 (2019).
38. Vellinga, M. & Wood, R. A. Global climatic impacts of a collapse of the Atlantic thermohaline circulation. *Climatic Change* **54**, 251–267 (2002).
39. Orihuela-Pinto, B., England, M. H. & Taschetto, A. S. Interbasin and interhemispheric impacts of a collapsed Atlantic Overturning Circulation. *Nat. Clim. Change* **12**, 558–565 (2022).
40. Zickfeld, K., Eby, M. & Weaver, A. J. Carbon-cycle feedbacks of changes in the Atlantic Meridional Overturning Circulation under future atmospheric CO₂. *Glob. Biogeochem. Cycles* **22**, GB3024 (2008).
41. Chikamoto, M. O. & DiNezio, P. Multi-century changes in the ocean carbon cycle controlled by the tropical oceans and the southern ocean. *Glob. Biogeochemical Cycles* **35**, e2021GB007090 (2021).
42. Boot, A. A., von der Heydt, A. S. & Dijkstra, H. A. Response of atmospheric pCO₂ to a strong AMOC weakening under low and high emission scenarios. *Clim. Dynamics* **62**, 7559–7574 (2024).
43. Willeit, M. & Ganopolski, A. Generalized stability landscape of the Atlantic Meridional Overturning Circulation. *Earth Syst. Dyn.* **15**, 1417–1434 (2024).
44. Curtis, P. E. & Fedorov, A. V. Collapse and slow recovery of the Atlantic Meridional Overturning Circulation (AMOC) under abrupt greenhouse gas forcing. *Clim. Dynamics* **62**, 5949–5970 (2024).
45. Willeit, M., Ganopolski, A., Robinson, A. & Edwards, N. R. The Earth system model CLIMBER-X v1. 0. Part 1: climate model description and validation. *Geoscientific Model Dev. Discuss.* **2022**, 1–69 (2022).
46. Willeit, M. et al. The Earth system model CLIMBER-X v1. 0–Part 2: The global carbon cycle. *Geoscientific Model Dev.* **16**, 3501–3534 (2023).
47. Zhang, R. et al. A review of the role of the Atlantic meridional overturning circulation in Atlantic multidecadal variability and associated climate impacts. *Rev. Geophysics* **57**, 316–375 (2019).
48. Talley, L. D., Reid, J. L. & Robbins, P. E. Data-based meridional overturning streamfunctions for the global ocean. *J. Clim.* **16**, 3213–3226 (2003).
49. Stewart, A. L., Chi, X., Solodoch, A. & Hogg, A. M. High-frequency fluctuations in Antarctic Bottom Water transport driven by southern ocean winds. *Geophys. Res. Lett.* **48**, e2021GL094569 (2021).
50. Nazarenko, L. S. et al. Future climate change under SSP emission scenarios with GISS-E2. 1. *J. Adv. Modeling Earth Syst.* **14**, e2021MS002871 (2022).
51. Kuhlbrodt, T. et al. On the driving processes of the Atlantic Meridional Overturning Circulation. *Rev. Geophys.* **45**, RG2001 (2007).
52. De Boer, A., Toggweiler, J. & Sigman, D. M. Atlantic dominance of the meridional overturning circulation. *J. Phys. Oceanogr.* **38**, 435–450 (2008).
53. Liu, W., Fedorov, A. V., Xie, S.-P. & Hu, S. Climate impacts of a weakened Atlantic meridional overturning circulation in a warming climate. *Sci. Adv.* **6**, eaaz4876 (2020).
54. Bellomo, K. & Mehling, O. Impacts and state-dependence of amoc weakening in a warming climate. *Geophys. Res. Lett.* **51**, e2023GL107624 (2024).
55. Fay, A. R. et al. Updated climatological mean δf CO₂ and net sea–air CO₂ flux over the global open ocean regions. *Earth Syst. Sci. Data* **16**, 2123–2139 (2024).
56. Gregor, L., Shutler, J. & Gruber, N. High-resolution variability of the ocean carbon sink. *Glob. Biogeochemical Cycles* **38**, e2024GB008127 (2024).
57. Gruber, N. et al. Oceanic sources, sinks, and transport of atmospheric CO₂. *Glob. Biogeochem. Cycles* **23**, GB1005 (2009).
58. Skinner, L., Menviel, L., Broadfield, L., Gottschalk, J. & Greaves, M. Southern Ocean convection amplified past Antarctic warming and atmospheric CO₂ rise during Heinrich Stadial 4. *Commun. Earth Environ.* **1**, 23 (2020).
59. Menviel, L., Spence, P. & England, M. H. Contribution of enhanced Antarctic Bottom Water formation to Antarctic warm events and millennial-scale atmospheric CO₂ increase. *Earth Planet. Sci. Lett.* **413**, 37–50 (2015).
60. Willeit, M. et al. Earth system response to Heinrich events explained by a bipolar convection seesaw. *Nat. Geosci.* **18**, 1159–1166 (2025).
61. Willeit, M., Ganopolski, A., Edwards, N. R. & Rahmstorf, S. Surface buoyancy control of millennial-scale variations in the Atlantic meridional ocean circulation. *Climate* **20**, 2719–2739 (2024).
62. Vettoretti, G., Ditlevsen, P., Jochum, M. & Rasmussen, S. O. Atmospheric CO₂ control of spontaneous millennial-scale ice age climate oscillations. *Nat. Geosci.* **15**, 300–306 (2022).
63. Malmierca-Vallet, I. et al. The impact of CO₂ and climate state on whether Dansgaard–Oeschger type oscillations occur in climate models. *Geophys. Res. Lett.* **51**, e2024GL110068 (2024).
64. Bauska, T. K., Marcott, S. A. & Brook, E. J. Abrupt changes in the global carbon cycle during the last glacial period. *Nat. Geosci.* **14**, 91–96 (2021).
65. Jochum, M. et al. Carbon fluxes during Dansgaard–Oeschger events as simulated by an Earth System Model. *J. Clim.* **35**, 5745–5758 (2022).
66. Meissner, K. J., Eby, M., Weaver, A. J. & Saenko, O. A. CO₂ threshold for millennial-scale oscillations in the climate system: implications for global warming scenarios. *Clim. Dyn.* **30**, 161–174 (2008).
67. Yu, J. et al. Millennial atmospheric CO₂ changes linked to ocean ventilation modes over past 150,000 years. *Nat. Geosci.* **16**, 1166–1173 (2023).
68. Stocker, T. F. & Schmittner, A. Influence of CO₂ emission rates on the stability of the thermohaline circulation. *Nature* **388**, 862–865 (1997).
69. Sarmiento, J. L., Gruber, N. Ocean biogeochemical dynamics. Princeton University Press: Princeton, NJ, 2006.
70. Gong, X., Liu, H., Wang, F. & Heuzé, C. Of Atlantic meridional overturning circulation in the CMIP6 project. *Deep Sea Res. Part II: Topical Stud. Oceanogr.* **206**, 105193 (2022).
71. Heuzé, C. North Atlantic Deep Water Formation and AMOC in CMIP5 models. *Ocean Sci.* **13**, 609–622 (2017).
72. Liu, W., Xie, S.-P., Liu, Z. & Zhu, J. Overlooked possibility of a collapsed Atlantic meridional overturning circulation in a warming climate. *Sci. Adv.* **3**, e1601666 (2017).
73. Obata, A. Climate–carbon cycle model response to freshwater discharge into the North Atlantic. *J. Clim.* **20**, 5962–5976 (2007).

74. Bozbiyik, A., Steinacher, M., Joos, F., Stocker, T. F. & Menviel, L. Fingerprints of changes in the terrestrial carbon cycle in response to large reorganizations in ocean circulation. *Climate* **7**, 319–338 (2011).
75. Nielsen, S. B., Jochum, M., Pedro, J. B., Eden, C. & Nuterman, R. Two-timescale carbon cycle response to an AMOC collapse. *Paleoceanogr. Paleoclimatology* **34**, 511–523 (2019).
76. Gatti, L. V. et al. Amazonia as a carbon source linked to deforestation and climate change. *Nature* **595**, 388–393 (2021).
77. Gatti, L. V. et al. Increased Amazon carbon emissions mainly from decline in law enforcement. *Nature* **621**, 318–323 (2023).
78. Aschwanden, A. et al. Contribution of the Greenland ice sheet to sea level over the next millennium. *Sci. Adv.* **5**, eaav9396 (2019).
79. Sinet, S., von der Heydt, A. S. & Dijkstra, H. A. Meltwater from the West Antarctic ice sheet tipping affects amoc resilience. *Sci. Adv.* **11**, eadw3852 (2025).
80. Edwards, N. R. & Marsh, R. Uncertainties due to transport-parameter sensitivity in an efficient 3-D ocean-climate model. *Clim. Dyn.* **24**, 415–433 (2005).
81. Willeit, M. & Ganopolski, A. Paladyn v1. 0, a comprehensive land surface–vegetation–carbon cycle model of intermediate complexity. *Geoscientific Model Dev.* **9**, 3817–3857 (2016).

Acknowledgements

M.W. is funded by the German climate modeling project PalMod supported by the German Federal Ministry of Education and Research (BMBF) as a Research for Sustainability initiative (FONA) (grant nos. 01LP1920B, 01LP1917D, 01LP2305B). N.W. is grateful for funding from the Center for Critical Computational Studies (C³S). The authors gratefully acknowledge the European Regional Development Fund (ERDF), the German Federal Ministry of Education and Research and the Land Brandenburg for supporting this project by providing resources on the high-performance computer system at the Potsdam Institute for Climate Impact Research. We thank the anonymous reviewers for their constructive and helpful comments.

Author contributions

D.N., J.R., and M.W. conceived and designed the research. D.N. carried out the modelling experiments, performed the analyses, and wrote the first draft of the manuscript. D.N., M.W., N.W., A.G., and J.R. discussed and interpreted the results and contributed to revising the manuscript.

Funding

Open Access funding enabled and organized by Projekt DEAL.

Competing interests

The authors declare no competing interests.

Additional information

Supplementary information The online version contains supplementary material available at <https://doi.org/10.1038/s43247-026-03427-w>.

Correspondence and requests for materials should be addressed to Da Nian.

Peer review information *Communications Earth and Environment* thanks the anonymous reviewers for their contribution to the peer review of this work. Primary Handling Editors: Weiqing Han and Alice Drinkwater. A peer review file is available.

Reprints and permissions information is available at <http://www.nature.com/reprints>

Publisher's note Springer Nature remains neutral with regard to jurisdictional claims in published maps and institutional affiliations.

Open Access This article is licensed under a Creative Commons Attribution 4.0 International License, which permits use, sharing, adaptation, distribution and reproduction in any medium or format, as long as you give appropriate credit to the original author(s) and the source, provide a link to the Creative Commons licence, and indicate if changes were made. The images or other third party material in this article are included in the article's Creative Commons licence, unless indicated otherwise in a credit line to the material. If material is not included in the article's Creative Commons licence and your intended use is not permitted by statutory regulation or exceeds the permitted use, you will need to obtain permission directly from the copyright holder. To view a copy of this licence, visit <http://creativecommons.org/licenses/by/4.0/>.

© The Author(s) 2026